

Journal of Materials Chemistry A

Accepted Manuscript



This is an *Accepted Manuscript*, which has been through the Royal Society of Chemistry peer review process and has been accepted for publication.

Accepted Manuscripts are published online shortly after acceptance, before technical editing, formatting and proof reading. Using this free service, authors can make their results available to the community, in citable form, before we publish the edited article. We will replace this *Accepted Manuscript* with the edited and formatted *Advance Article* as soon as it is available.

You can find more information about *Accepted Manuscripts* in the [Information for Authors](#).

Please note that technical editing may introduce minor changes to the text and/or graphics, which may alter content. The journal's standard [Terms & Conditions](#) and the [Ethical guidelines](#) still apply. In no event shall the Royal Society of Chemistry be held responsible for any errors or omissions in this *Accepted Manuscript* or any consequences arising from the use of any information it contains.

Laser induced instantaneous gelation: Aerogels for 3D printing

Shaukat Saeed^{a,c}, Rola Al-Sobaihi^a, Massimo F. Bertino^{b*}, Lauren S. White^b, Khaled M. Saoud^{1a*}

Abstract

We present synthesis of polymer cross-linked silica aerogels in a matter of seconds by illuminating the solution of TEOS, Hexanedioldiacrylate, Eosin and amine with laser beam ($\lambda=532$). The heat of polymerization triggers gelation instantly. We demonstrate printing of 3D letters on different substrates using this technique. The physical properties of the 3D printed samples are comparable to conventionally prepared cross-linked silica aerogels, i.e., shrinkage (10.4%), density (0.56 g/cm³), Young's modulus (81.3 MPa) and BET surface area (155.3 m²/g). An important aspect of this rapid gelation is that it allows 3D printing / lithography of reinforced silica aerogel without using a mould.

^a Department of Liberal Arts and Sciences, Virginia Commonwealth University, Doha, Qatar.

^b Department of Physics, Virginia Commonwealth University, Richmond, VA 23060, USA.

^c Department of Metallurgy and Materials Engineering, Pakistan Institute of Engineering and Applied Sciences (PIEAS), Islamabad-45650, Pakistan.

* Corresponding authors: s2kmsaou@vcu.edu and mfbertino@vcu.edu

1. Introduction

Lightweight materials with adequate mechanical properties are highly desired for various structural applications. It is expected that in the near future every structure, simple or complex, will be fabricated using 3D printing technology. Various materials being explored for 3D printing are laser sintered metals, photo-crosslinked polymers and extruded molten polymers. However, all these materials have inherently high densities which render them unsuitable for lightweight structures. Here, we demonstrate that instantaneous gelation leading to mechanically strong and ultra-lightweight silica aerogels offer a new direction for 3D industry to fabricate lightweight 3D structures with complex geometries using visible light emitting low power laser.

Silica aerogels are highly porous materials, composed of over 90% air and rest as silica network structure. This unique composition and structure impart peculiar properties such as high surface area, very low bulk density and low thermal conductivity. They find applications in catalysis^{1, 2}, adsorption³, thermal insulation^{4, 5}, environmental remediation⁶ and space exploration⁷. Aerogels, however, could not find deep penetration into the market as structural material for a number of reasons. They are fragile, synthesis requires several steps, and drying is complex and time-consuming. Fragility issues have been addressed in large part by the Leventis group^{8, 9}, who cross-linked the skeletal oxide nanoparticles with a conformal polymer coating. Crosslinking increases mechanical strength by orders of magnitude without overly compromising porosity. The strengthening strategies include use of higher functionality cross-linker, selective crosslinking of the regions subject to shear and mechanical stress, and specific patterning like honeycomb structures to increase compressive strength of aerogels along the load-bearing direction¹⁰⁻¹². Drying is another issue affecting aerogel applications. To reduce capillary forces (which cause cracking during drying), supercritical CO₂ is typically employed. However, supercritical CO₂ drying requires multiple, time-consuming solvent exchanges, which make the method unpractical for large-scale applications. Drying issues have been partially addressed by

Schwertfeger et al.¹³, and more recently, the groups of Anderson and Carroll¹⁴ and our own group¹⁵ developed drying techniques employing supercritical ethanol that eliminated time consuming solvent exchange steps.

Even with these improvements, however, a processing bottleneck remains, and that is the synthesis of wet gels. Gelation times depend strongly on precursor concentration and pH, and in most cases are on the order of tens of minutes to hours. After gelation, wet gels need to be cured for hours to days to strengthen the silica network. Here, we present a method that allows instantaneous fabrication of alcogel monoliths and demonstrate 3D printing of alphabetical letters. To the best of our knowledge, there is no report on rapid fabrication of mechanically strong aerogels capable of printing 3D structures.

In our method, a precursor solution of an alkoxide, a monomer and a visible-light photo-initiator is prepared and illuminated with a 2 watt laser source. Illumination initiates free-radical polymerization. The heat of polymerization, in turn, induces gelation. Synthesis employs the ethanol-water azeotrope as a gelation solvent, thus, wet gels can be dried immediately after gelation using the technique developed by our group¹⁵. Here, we demonstrate manual printing of 3D letters on different substrates like laminated paper, glass slide and silicon wafer using masking techniques, and also printing of a 50 μm thick line on glass substrate through direct shining of laser on the liquid mixture without any mask. The samples were then dried at supercritical conditions along with substrate and as self-standing objects. The technique may be extended to fabricate more complex 3D structures, thin film or any patterned objects from the ultralight aerogels.

2. Experimental

2.1 Chemicals

Reagent-grade tetraethyl orthosilicate (TEOS), aluminum chloride hexahydrate ($\text{AlCl}_3 \cdot 6\text{H}_2\text{O}$), trimethoxysilylpropyl methacrylate (TMSM), methyldiethanoethylamine (Amine), Eosin Y were purchased from Acros Organics. Hexanedioldiacrylate (HDDA) was purchased from Sigma-Aldrich. All reagents were used as-received. The ethanol–water azeotrope mixture

(containing 4.4% water and 95.6% pure ethanol by volume) was used as gelation solvent and as supercritical fluid in the drying process for the samples prepared. Unless stated otherwise, all references to ethanol in this manuscript refer to ethanol–water azeotrope.

2.2 Supercritical drying of alcogels

We followed the same procedure for supercritically drying the samples as reported in our recent publication¹⁵. Briefly, the alcogels with or without their substrate were placed inside the supercritical dryer, a Parr Instruments model 4602 pressure vessel with a capacity of 2 litres. The pressure vessel was equipped with a thermal well and it was heated by three ceramic heaters, each with a power of 800 W. Heating rates were controlled by varying the power delivered to the heaters with a Variac. To prevent solvent evaporation from the alcogels before the supercritical point was reached, an excess volume (500 ml) of ethanol was poured into the drying vessel. The pressure vessel was heated to reach the supercritical temperature and pressure of the ethanol–water azeotrope mixture, kept at supercritical conditions for 20 minutes and then vented.

2.3 Characterization

FTIR Spectroscopic measurements were carried out using a Thermo Scientific Nicolet 6700. A smart iTR diamond ATR accessory was used. Background was subtracted each time while obtaining data from ATR accessory. For each sample, 64 scans were taken with data spacing of 0.482 cm^{-1} and a resolution of 4 cm^{-1} .

CPMAS-TOSS solid-state NMR spectra were acquired on a Bruker DRX300WB spectrometer equipped with a 7 mm CPMAS probe. Each sample was packed into a 7 mm Zirconia rotor with Kel-F cap and then spun at 5 kHz at room temperature. The operating frequency was 75.48 and 59.62 MHz for ^{13}C and ^{29}Si , respectively. The contact time was 5 ms for ^{29}Si and 1 ms for ^{13}C and repetition time was 2 s for both nuclei. The measurement time was sample dependent because of number of scans ranging from 300 to 2000 for ^{13}C and 1000 to 2000 for ^{29}Si . A line broadening of 60 Hz (^{13}C) and 100 Hz (^{29}Si) for each was applied before Fourier Transformation. Chemical shift was externally referenced to glycine (C=O carbon at 176.03 ppm) and DSS (sodium salt of 2,2-dimethyl-2-silapentane-5-sulphonic acid, ^{29}Si at 0 ppm).

For compression testing, we employed an Insight 30 using a 50 N load cell and compression velocity $0.254 \text{ cm min}^{-1}$. The self-standing samples (without substrate) were placed on the stage horizontally and were tested.

Surface areas were measured with a Micromeritics ASAP 2020 analyzer. Samples with an average weight of 40 mg were outgassed in vacuum for 24 hours at $120 \text{ }^\circ\text{C}$. In each test, 5 adsorption/desorption points were taken with 3 minutes of equilibration time between each measurement and tolerance of 0 at 77.2 K (sample holder submerged in liquid nitrogen). The surface area values are calculated according to the BET model using these points of the adsorption curve.

Scanning Electron Microscope (Model: Hitachi SU-70) was used to image aerogel samples. The nominal thickness of the samples was $\leq 1 \text{ mm}$ and were placed on carbon conductive tabs adhered to the sample mount. A strip of adhesive copper tape, connecting the sample and sample mount, was placed in contact with each piece of aerogel to avoid charging during imaging. The samples were sputter coated for 30 seconds with gold and then imaged. High Resolution Transmission electron microscopy (HRTEM; model: JEOL JEM-2100F) was used for the morphological characterization of the samples.

2.4 Sample Preparation

For alcogel fabrication, two solutions were prepared and kept in separate polypropylene containers before mixing. Solution A was prepared by mixing 0.88 ml (4.0 mmol) of tetraorthosilicate (TEOS), 0.04 ml (0.2 mmol) of trimethoxysilylpropyl methacrylate (TMSP) and 1.85 ml of ethanol-water azeotrope mixture in which $\text{AlCl}_3 \cdot 6\text{H}_2\text{O}$ had been dissolved (concentration: 1.4 mmol/l). Solution B was prepared by mixing 0.15 ml (0.87 μmol) of Eosin Y, 0.05 ml (0.434 mmol) of methyldiethanoethylamine (amine), 1.12 ml (5.0 mmol) of hexanedioldiacrylate (HDDA) and 0.5 ml ethanol-water azeotrope. Eosin Y, which absorbs in the green region of the visible spectrum, was used as the photo-initiator and the tertiary amine acted as co-initiator and pH modifier. A 2 Watt, continuous wave, diode-pumped solid-state laser emitting light at a wavelength of 532 nm was employed in this study. Upon light absorption, charge is transferred between Eosin Y and the amine, resulting in a reduced radical dye and a radical capable of initiating polymerization^{16, 17}. During 3D printing, gelation was almost

instantaneous upon irradiation. Solution preparation and 3D printing process is illustrated in Figure 1.

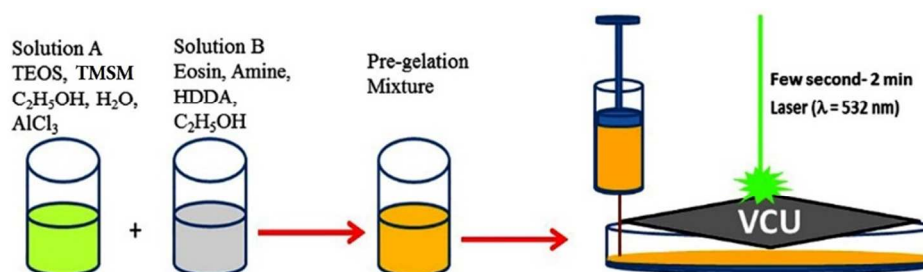


Figure 1: Schematics for 3D printing of aerogel materials using green Laser light.

Layer by layer technique was used for 3D printing where solution mixture was added to a Petri dish covered with a stencil mask. Light was shined through the cut-out holes of the letters to gel the solution underneath and then another quantity of mixture was added. Light was shined again and it was repeated until desired thickness of the letters was achieved. The aerogel material showed good adhesion with substrate and good stiffness as self-standing object.

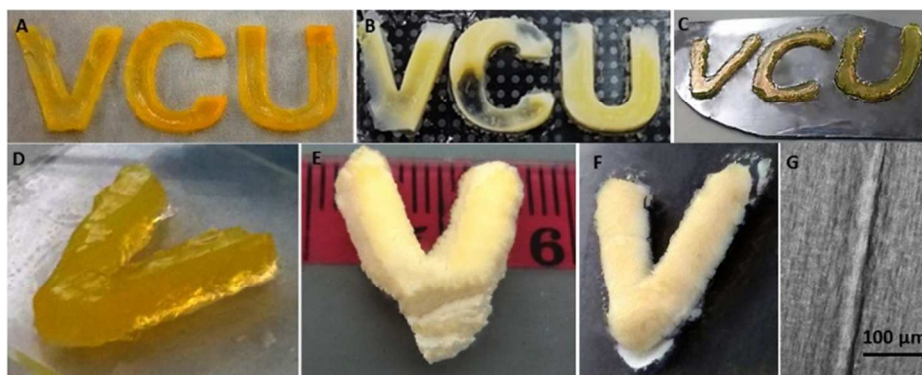


Figure 2: Shows letters printed using mask, (a) on laminated paper, (b) on glass, (c) on silicon wafer, (d) on glass, and letter “V” was dried at supercritical conditions and shown as: (e) without substrate, (f) on glass substrate, whereas (g) shows a line printed without mask on glass. The typical thickness of the letters is 2-4 mm whereas each letter has dimensions of 12 mm x 15 mm.

3. Results and Discussion

The key of our fabrication method is instantaneous gelation that spread within seconds to whole exposed area. This rapid gelation can be explained by considering the strong temperature dependence of the gelation process. While alkoxide hydrolysis is exothermic, condensation is endothermic¹⁸ and it is strongly accelerated when the temperature is increased. For example, the group of Sakka¹⁹ reported a decrease in gelation time of more than one order of magnitude when the temperature was raised from 25 to 80 °C. In our case, polymerization likely provided sufficient heat locally to raise the temperature and accelerate the gelation. The theoretical heat evolved when a methacrylate double bond converts is $\Delta H = 13.1 \text{ kcal/mol}$ ^{20, 21}. This value which agrees well with experimental determinations, which range from 12.2 to 20.2 kcal/mol. The temperature increase of the gelation solution can be estimated as $\Delta T = (n_{\text{mono}} * \Delta H) / (m * C_p)$, where n_{mono} is the number of monomer moles, m the mass of the solvent and C_p the heat capacity of the solvent. Using the value of ΔH discussed above and the reagent concentration for this system, we obtain $\Delta T \sim 70 \text{ K}$, which explains the immediate gelation of the silica precursor solution once polymerization is triggered. Alternatively, one can consider that the energy required by the condensation reaction is between 0.28 and 2.8 kcal/mol^{18, 22-24}. This energy is about one order of magnitude lower than the energy ΔH liberated by the double bond conversion, and this also explains the observed rapid gelation.

The direct heating by the laser beam may be considered a reason to cause gelation. However, based on our previous experience, we do not think that direct heating played a relevant role in this case. In previous work on quantum dot lithography²⁵, for example, direct laser heating was employed to induce chemical reactions. However, a temperature increase was noticed only in the immediate vicinity (40 to 80 microns) when an infrared laser was employed and the laser was focused with a lens. In the present study, the laser was not focused and green light was employed, which does not cause heating as infrared light do.

3.1 FTIR analysis

FTIR analysis (Figure 3) was performed using Thermo Scientific Nicolet 6700 machine on the supercritically dried sample to confirm formation of both silica and polyacrylate structures. The spectrum shows presence of a relatively large band at 1730 cm^{-1} which is attributed to the C=O

stretch vibrations whereas vibrations of C–O from the same ester groups of the polyacrylate appears at 1060 cm^{-1} . The absence of a band around 1640 cm^{-1} which corresponds to C=C (acrylic double bond) indicate formation for polyacrylate and engagement of TMSM through its acrylic group.

The presence of bands maxima at positions 1160 , 1090 – 1060 , 980 and 810 cm^{-1} confirms presence of silica network structures in the system. The bands centred around 1160 and 1090 – 1060 cm^{-1} correspond to the intense silicon–oxygen covalent bonds vibrations that confirm the formation of silica network. The absorption band around 980 cm^{-1} corresponds to in-plane stretching vibrations of Si–O of the silanol Si–OH groups²⁶. The bands appearing around 1090 cm^{-1} and the shoulder at around 1200 cm^{-1} are assigned respectively to the transversal optical and longitudinal optical modes of the Si–O–Si asymmetric stretching vibrations²⁷. The band at 800 cm^{-1} reflects symmetric stretching vibrations of Si–O–Si²⁸. The comparison of the spectra show formation of silica network and polymerization of HDDA monomer took place in both samples.

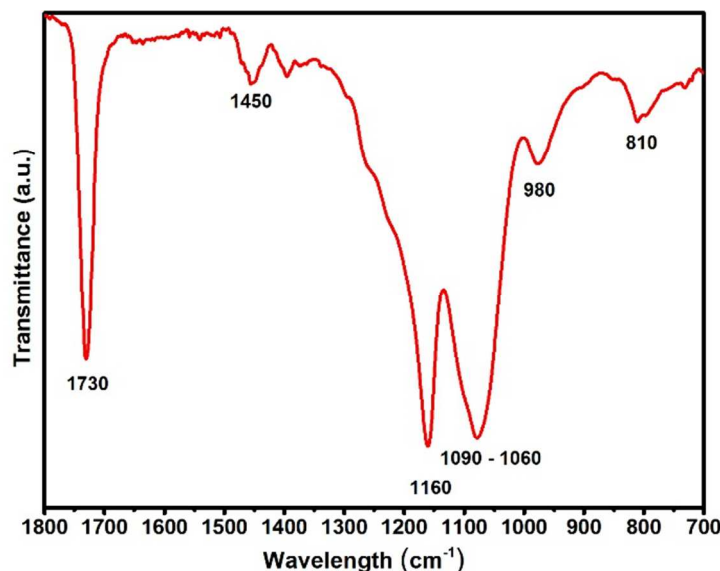


Figure 3: FTIR spectrum of 3D printed samples after supercritical drying showing formation of silica network and acrylate polymer.

3.2 NMR analysis

Solid-state NMR analysis was performed on the samples using Bruker DRX300WB spectrometer to further confirm the formation of both network structures and to find out any anomaly due to incomplete hydrolysis, condensation or polymerization during extraordinary fast

fabrication of aerogels. The spectrum obtained using ^{29}Si and ^{13}C modes are presented in the Figures 4. The ^{29}Si spectra exhibit two major characteristic peaks at -103.04 ppm due to silanol and -111.52 ppm due to siloxane structures. A very small peak at -67.67 ppm points toward low concentration of tridentate bonding of TMSM to silica²⁹ which corresponds to the small amount of TMSM in the system. Absence of a peaks at -52 ppm and -59 ppm confirms presence of almost no mono or bidentate bonding of TMSM or TEOS to the silica framework which further confirm completion of hydrolysis and condensation processes³⁰. All these observations indicate completion of hydrolysis and condensation reactions leading to formation of silica network structure in all samples.

The ^{13}C spectrum of the samples show peaks at 26.22 , 28.26 , 40.26 , 64.30 , and 174.09 ppm which originate from the aliphatic carbons of HDDA's acrylate polymer. The shift in strong signal of carbonyl carbon of HDDA from 167 ppm to 174.09 ppm in the SC dried sample confirms formation of acrylate polymer. The detailed discussion has been reported in our recent publication¹⁵ whereas here, the discussion is limited only to the confirmation of conversion of precursor and monomer to polymer crosslinked-silica structures due to laser illumination.

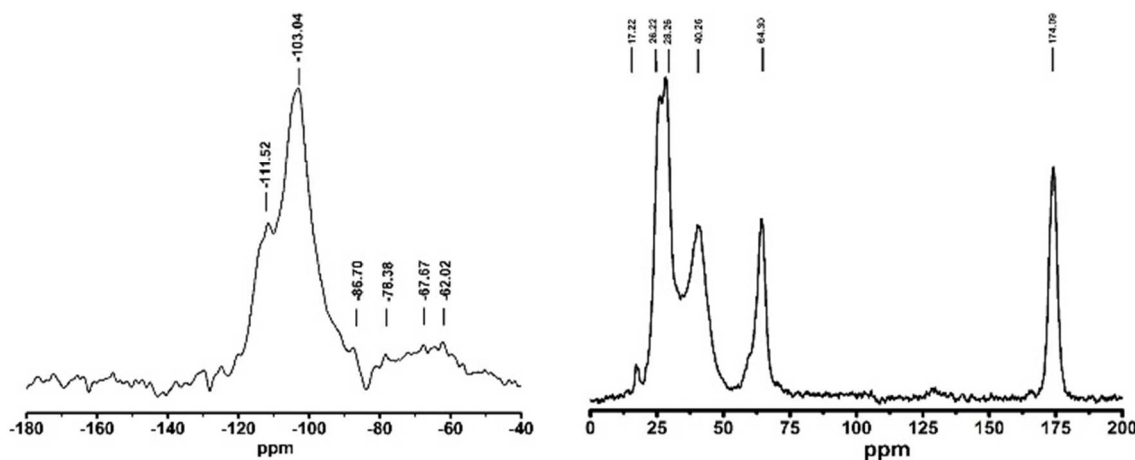


Figure 4: Solid-state NMR ^{29}Si (-180 to -40 ppm) and ^{13}C spectra (0 to 200 ppm) for supercritically-dried cross-linked aerogels.

3.3 Morphological Analysis

Morphological evaluation of the aerogel materials was performed using SEM and TEM. The SEM and TEM micrographs for the 3D printed letters, depicted in Figure 5, clearly show formation and arrangement of secondary particles with a diameter between about 10 and 30 nm,

as well as a clearly defined pore structure. Primary particles could not be observed in SEM because of the polymer cross-linking, as customary for this class of materials.

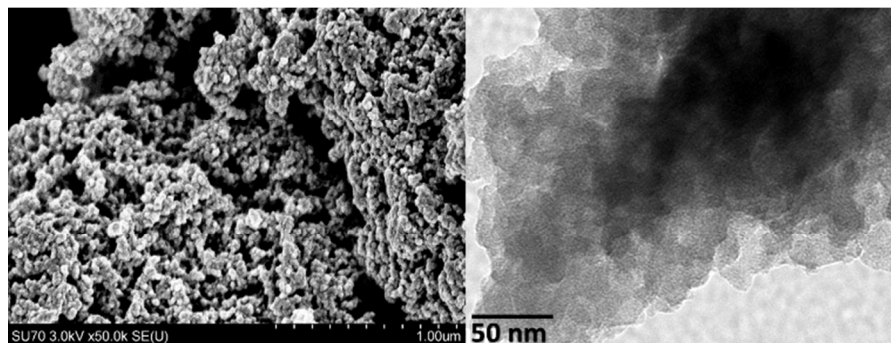


Figure 5: SEM (left) and TEM (right) micrographs of the aerogel samples showing cross-linked secondary particles and a nano-porous structure.

3.4 Physical Properties

Mechanical properties were measured on Insight 30 and surface area using Micromeritics ASAP 2020 analyser. The average values of physical properties for the 3D printed aerogel samples are: shrinkage (10.4%), density (0.56 g/cm^3), modulus (81.3 MPa) and BET surface area ($155.3 \text{ m}^2/\text{g}$). All these values are within the range expected for cross-linked aerogels³¹. Thus, instantaneous gelation leading to aerogels show comparable properties in addition to ease in fabrication.

4. Conclusions

It can be concluded that polymer crosslinked aerogel materials prepared instantly by irradiating a liquid mixture of an alkoxy silane, a monomer and a photo-initiator can be used to print 3D objects. Irradiation leads to instantaneous polymerization and gelation. Internal heat changes involved in the crosslinking reactions play an important role to overcome the activation energy barrier for condensation reactions that leads to instantaneous formation of silica network structure. Comparable physical properties including such as density, modulus, shrinkage and surface area has been observed for the materials crosslinked and gelled within seconds than those prepared in hours or days using conventional procedures. Significant improvement in the fabrication process of photo-crosslinked aerogel materials is expected to replace high density structural materials being used

for 3D printing or for other such applications with ultra-low density crosslinked aerogel materials.

Acknowledgements

This publication was made possible by an NPRP award [NPRP 6 - 892 - 1 - 169] from the Qatar National Research Fund (a member of The Qatar Foundation). We also thank the US National Science Foundation for an instrumentation award (CHE-1337700) which was used to purchase the Raman spectrometer used for characterization. We are thankful to Mr. Timothy Dexter De Voe from Digital Fabrication Lab at VCU Qatar for fabricating stencils for this work.

References

1. S. Maury, P. Buisson, A. Perrard and A. C. Pierre, *Journal of Molecular Catalysis B-Enzymatic*, 2004, 29, 133-148.
2. M. Schneider and A. Baiker, *Catalysis Reviews: Science and Engineering*, 1995, 37, 41.
3. L. W. Hrubesh, P. R. Coronado and J. H. Satcher, *Journal of Non-Crystalline Solids*, 2001, 285, 328-332.
4. G. S. Kim and S. H. Hyun, *Journal of Non-Crystalline Solids*, 2003, 320, 125-132.
5. R. Baetens, B. P. Jelle and A. Gustavsen, *Energy and Buildings*, 2011, 43, 761-769.
6. B. Heckman, L. Martin, M. F. Bertino, N. Leventis and A. T. Tokuhiko, *Separation Science and Technology*, 2008, 43, 1474-1487.
7. S. M. Jones, *Journal of Sol-Gel Science and Technology*, 2007, 44, 255-258.
8. N. Leventis, C. Sotiriou-Leventis, G. H. Zhang and A. M. M. Rawashdeh, *Nano Letters*, 2002, 2, 957-960.
9. N. Leventis and H. Lu, in *Aerogels Handbook*, eds. M. A. Aegerter, N. Leventis and M. M. Koebel, Springer, New York, 2011, ch. 13, pp. 251-285.
10. L. S. White, M. F. Bertino, S. Saeed and K. Saoud, *Microporous and Mesoporous Materials*, 2015, 217, 244 - 252.

11. C. Wingfield, L. Franzel, M. F. Bertino and N. Leventis, *Journal of Materials Chemistry*, 2011, 21, 11737-11741.
12. L. Franzel, C. Wingfield, M. F. Bertino, S. Mahadik-Khanolkar and N. Leventis, *Journal of Materials Chemistry A*, 2013, 1, 6021-6029.
13. M. Schmidt and F. Schwertfeger, *Journal of Non-Crystalline Solids*, 1998, 225, 364-368.
14. A. M. Anderson, C. W. Wattlely and M. K. Carroll, *Journal of Non-Crystalline Solids*, 2009, 355, 101-108.
15. L. S. White, M. F. Bertino, G. Kitchen, J. Young, C. Newton, R. Al-Soubaihi, S. Saeed and K. Saoud, *Journal of Materials Chemistry A*, 2015, 3, 762-772.
16. H. J. Avens and C. N. Bowman, *Journal of Polymer Science Part a-Polymer Chemistry*, 2009, 47, 6083-6094.
17. D. M. Burget, C.; Fouassier, J. P., *Polymer* 2004, 45, 7.
18. J. Matsuoka, M. Numaguchi, S. Yoshida and N. Soga, *Journal of Sol-Gel Science and Technology* 2000, 19, 4.
19. S. Sakka and K. Kamiya, *Journal of Non-Crystalline Solids*, 1982, 48, 16.
20. K. Miyazaki and T. Horibe, *Journal of Biomedical Materials Research*, 1988, 22, 13.
21. K. Horie, A. Otagawa, M. Muraoka and I. Mita, *Journal of Polymer Science: Polymer Chemistry Edition*, 1975, 13, 10.
22. F. D. Osterholtz and E. R. Pohl, *Journal of Adhesion Science and Technology*, 1992, 6, 23.
23. Z. Lasocki, *Bulletin of the Polish Academy of Sciences - Technical Sciences*, 1963, 11, 6.
24. J. Chojnowski and S. Chrzczonowicz, *Bulletin of the Polish Academy of Sciences - Technical Sciences*, 1965, 13, 5.
25. M. Bertino, in *Aerogels Handbook*, eds. M. A. Aegerter, N. Leventis and M. M. Koebel, Springer, New York, 2011, ch. 19, pp. 403-418.
26. N. O. Gopal, K. V. Narasimhulu and J. L. Rao, *Spectrochimica Acta Part A: Molecular and Biomolecular Spectroscopy*, 2004, 60, 8.

27. A. Duran, C. Serna, V. Fornes and J. M. F. Navarro, *Journal of Non-Crystalline Solids*, 1986, 82, 9.
28. C. J. Brinker and G. W. Scherer, *Sol-gel Science. The Physics and Chemistry of Sol-gel Processing*, Academic, New York, 1990.
29. L. N. Lewis, T. A. Early, M. Larsen, E. A. Williams and J. C. Grande, *Chemistry of Materials*, 1995, 7, 7.
30. S. Ek, E. I. Iiskola, L. Niinistö, J. Vaittinen, T. T. Pakkanen and A. Root, *The Journal of Physical Chemistry B*, 2004, 108, 10.
31. H. Lu, H. Luo and N. Leventis, in *Aerogels Handbook*, eds. M. A. Aegerter, N. Leventis and M. M. Koebel, Springer, New York, 2011, ch. 22 pp. 499 - 535.